Guidelines for measuring and analysing continuous stope closure behaviour in deep tabular excavations

Author

D.F. Malan - CSIR Miningtek

The Safety in Mines Research Advisory Committee

(SIMRAC)

August 2003

SIMRAC

Published by The Safety in Mines Research Advisory Committee (SIMRAC) Braamfontein Centre, 23 Jorissen Street, Braamfontein 2001, South Africa.

ISBN 1-919853-10-3

TABLE OF CONTENTS

INTRODUCTION

This guide was produced in response to a need identified in the South African gold mining industry for a better understanding of the closure behaviour of tabular excavations. Although references to closure measurements can be found dating back to the early 1930's, research in the SIMRAC fundamental projects GAP332 and GAP601b indicated that continuous closure recordings contain much important data which is lost with the traditional method of closure measurement (which consists of installing closure pegs and taking manual readings on a daily basis or less frequently).

The rate of closure is a very important parameter for support design and therefore impacts indirectly on safety. Continuous closure measurements also appear to be useful to identify different geotechnical areas and the hazards associated with each area. The objective of this guide is therefore to:

- create awareness of the need to do continuous closure measurements on a more regular basis,

- standardise the closure terminology used in the industry,
- illustrate the effect of mining rate on the rate of closure,
- highlight the effect of measurement position on the rate of closure.
- Illustrate the value of the closure ratio (CR) parameter to identify different geotechnical areas and hazardous conditions.

As the main objective of this book is to create an awareness of the value of continuous closure measurements, some of the more complex mathematical calculations are given in the Appendix and not in the main sections of the book.

TERMINOLOGY

Owing to much confusion surrounding closure terminology, the following definitions are introduced. Note that the definitions of *closure* and *convergence* below do not agree with the original terminology proposed by the ISRM in 1975. As the meaning of these words in reports and publications in the South African industry has changed with time, it is considered more appropriate to use the definitions given below.

- ***Closure*:** Relative movement of the hangingwall and footwall normal to the plane of the excavation (Figure 1).
- ***Ride*:** Relative movement of the hangingwall and footwall parallel to the plane of the excavation (Figure 1). It should be noted that for a dipping tabular excavation in three dimensions, the ride consists of two components namely ride in the strike direction and ride in the dip direction. In some cases an apparent ride component is also observed if the fractured rock of the footwall moves into the strike and dip gullies. This is very common on the Vaal Reef (Roberts, 2003)

- ***Convergence*:** Elastic component of closure. For deep tabular stopes, the closure is the sum of the convergence and inelastic movements caused by fracturing and the slip and opening of discontinuities such as bedding planes.

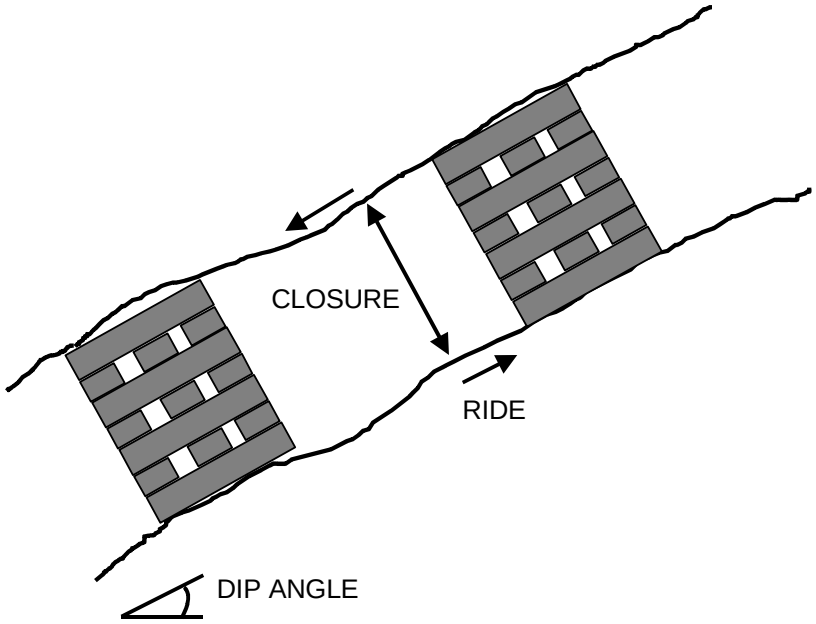

Figure 1. Definition of closure and ride.

- ***Long period closure measurements*:** Discrete closure measurements with a typical interval of 24 hours or longer between successive data points. These measurements are commonly plotted as a function of distance to face or time (usually in days or months). Figures 2 and 3 illustrate some examples. Note that if closure is plotted as a function of distance to face, the graph does not go through the origin as the closure instruments are always installed some distance behind the face. The data in

Figures 2 and 3 was recorded by closure stations at a fixed location in a panel and, with time, the face moved away from the measurement point due to regular blasting. These results can be misleading as the curves are a complex aggregate of face position changes and the time-dependent behaviour of the rock.

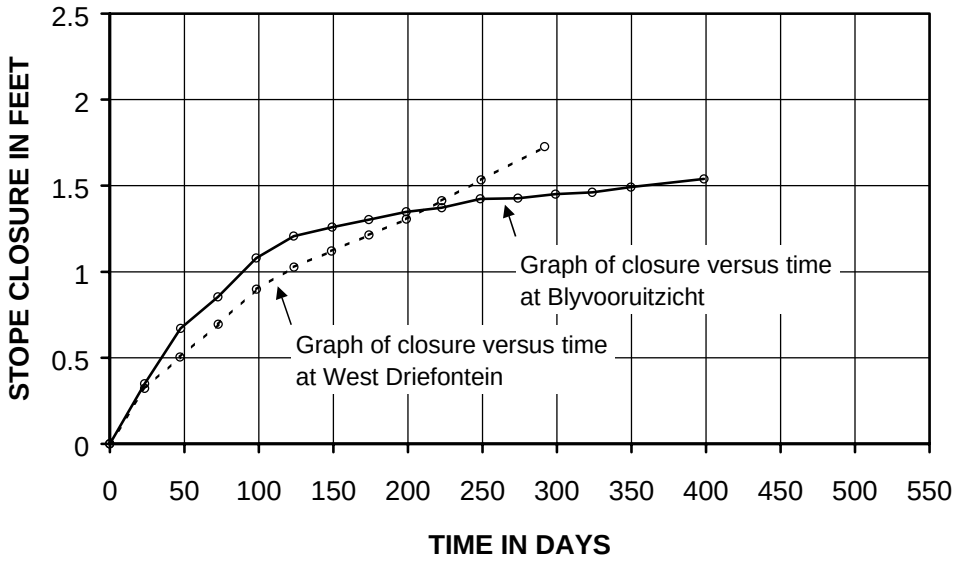

Figure 2. Typical closure curves obtained from long period measurements (after Wiggill 1965). In this example the closure is plotted as a function of time.

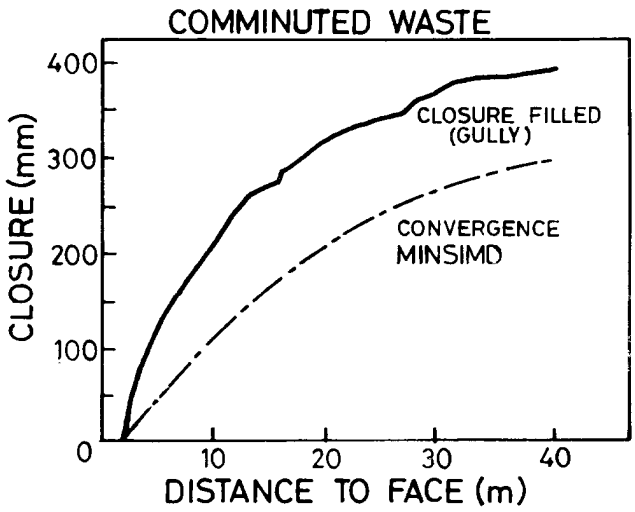

Figure 3. A typical closure curve obtained from long period measurements where the closure is plotted as a function of distance to face (after Gürtunca & Adams 1991).

- ***Continuous closure measurements*:** Closure recorded in a continuous fashion with suitable instrumentation such as clockwork closure meters. Closure collected with electronic data loggers with a sample frequency of greater than 1 sample/15 minutes will also be referred to as continuous. These measurements are always plotted as a function of time (usually in minutes or hours). An example is given in Figure 4. Note that the effects of changes in geometry, the time-dependent behaviour and seismic events are clearly distinguishable.
- ***Time-dependent closure*:** Slow ongoing closure observed between successive blasts when there is no

change in the mining geometry. This consists of a primary and steady-state phase as indicated in Figure 5.

- ***Primary closure phase*:** This is the component of time-dependent closure following a blast and is characterised by a period (≈ 3 to 5 hours) of decelerating rate of closure. It is also observed after large seismic events.
- **Steady-state closure:** The component of time-dependent closure following the primary closure phase (see Figure 5). The rate of steady-state closure appears to be constant in the short term but it gradually decreases when there is no blasting or seismic activity.

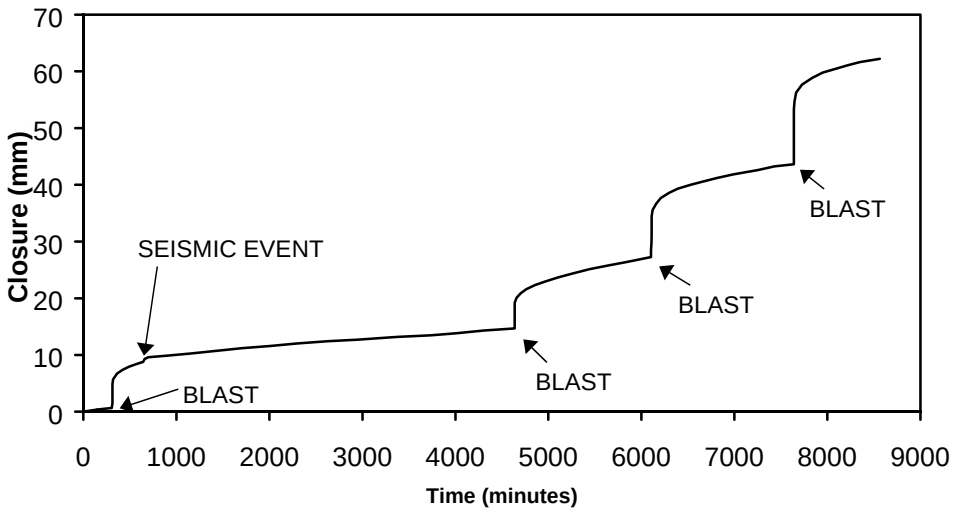

Figure 4. An example of continuous closure data collected in a VCR stope where the hangingwall consists of hard lava. Note that the unit of time in this figure is minutes, while it is days in Figure 2.

- ***Instantaneous blast closure*:** The instantaneous closure component occurring at blasting time (Figure 5). Due to the delays in the detonation sequence between adjacent blast holes in the face, this closure phase is not really instantaneous but can last for several minutes.

- ***Instantaneous seismic closure*:** The instantaneous closure component occurring during a seismic event. Similar to the blast closure, the instantaneous seismic closure is followed by a primary and steady-state closure phase.

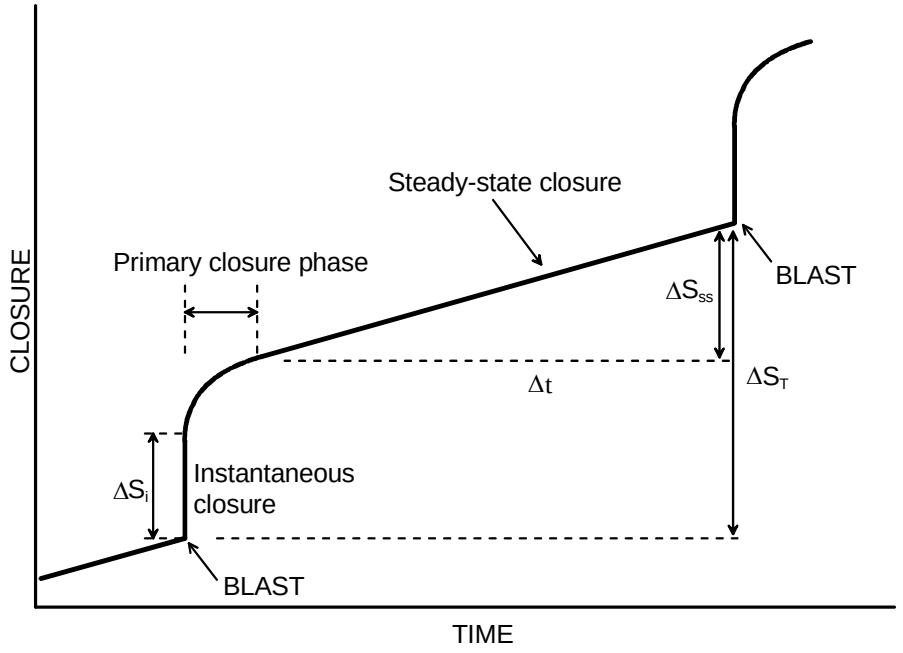

Figure 5. Typical continuous stope closure after blasting and the definition of closure terms.

- ***Rate of steady-state closure*:** Defined as

$$\dot{S}_{SS} = \frac{\Delta S_{SS}}{\Delta t} \quad (1)$$

where ΔS_{ss} is the increase in steady-state closure over the period Δt (see Figure 5). As the rate of steady-state closure gradually decreases in the absence of blasting activity, it is important to mention the period used for the calculation. The period Δt is often taken from six hours after the blast (to avoid the effect of the primary phase) to 24 hours after the blast (or until the next blast occurs, whichever comes first).

- ***Closure ratio*:** The ratio of the instantaneous blast closure to total closure following a blast. To avoid to risk of making inappropriate conclusions about sudden unexpected increases in closure ratio, this parameter is only defined for the closure following a blast and not for a seismic event.

UNITS FOR SPECIFYING RATE OF CLOSURE

Some confusion still prevails with regards to the most appropriate units to use when specifying rate of closure. Units currently in use are ***mm/m*** (amount of closure per meter of face advance) and ***mm/day***. This problem arises because measured closure consists of two components namely:

- closure due to enlargement of the excavation (the face moving away from the closure meter due to blasting)
- closure due to time dependent movements (creep) of the rockmass when there is no mining activity

As will be shown later in this guide, the time-dependent closure components are very large in some geotechnical areas of the gold mining industry and can therefore not be ignored.

Unfortunately the unit ***mm/m*** implies that closure is not a function of time while for the unit ***mm/day***, the effect of geometrical changes (face advance) is not directly accounted for. Both of these units should therefore be treated with caution. When referring to rate of closure in mm/m, it is important to specify the mining rate as well, while

for mm/day, the amount of face advance and the mining cycle (i.e. two day cycle or four day cycle) during the period of measurement should be specified.

To introduce a standard, it is suggested that the unit mm/m, together with the mining rate for which this particular value of closure rate is applicable, always be used. The unit mm/m is preferred as it is more convenient for the support design, while a method has also been developed to estimate the effect of mining rate on rate of closure expressed in mm/m (see Appendix A). The effect of mining rate on rate of closure (in mm/m) and how to estimate it for different mining rates is further discussed on page 17.

CONTINUOUS CLOSURE PROFILES IN DIFFERENT GEOTECHNICAL AREAS

From the analysis of closure measurements conducted in the SIMRAC projects GAP332, GAP601b and GAP852, it became clear that significant differences exist between the continuous closure profiles of different geotechnical areas. Figure 6 compares continuous closure profiles of two areas experiencing significantly different rock mass behaviours. The two experimental sites were approximately at the same depth and for these specific data sets, the closure instruments were approximately at the same distance from the face. Note that after three days of measurement, the total closure of the two areas are approximately similar. The following important differences are, however, noted. The closure behaviour of the Ventersdorp Contact Reef (hard lava) is characterised by a large instantaneous jump after blasting followed by a low steady-state closure rate. In contrast, for the experimental site in the Vaal Reef, the closure is characterised by a small instantaneous jump after blasting followed by a high rate of closure. Closure measurements of the VCR with a soft lava hangingwall indicated behaviour similar to that of the Vaal Reef in Figure 6.

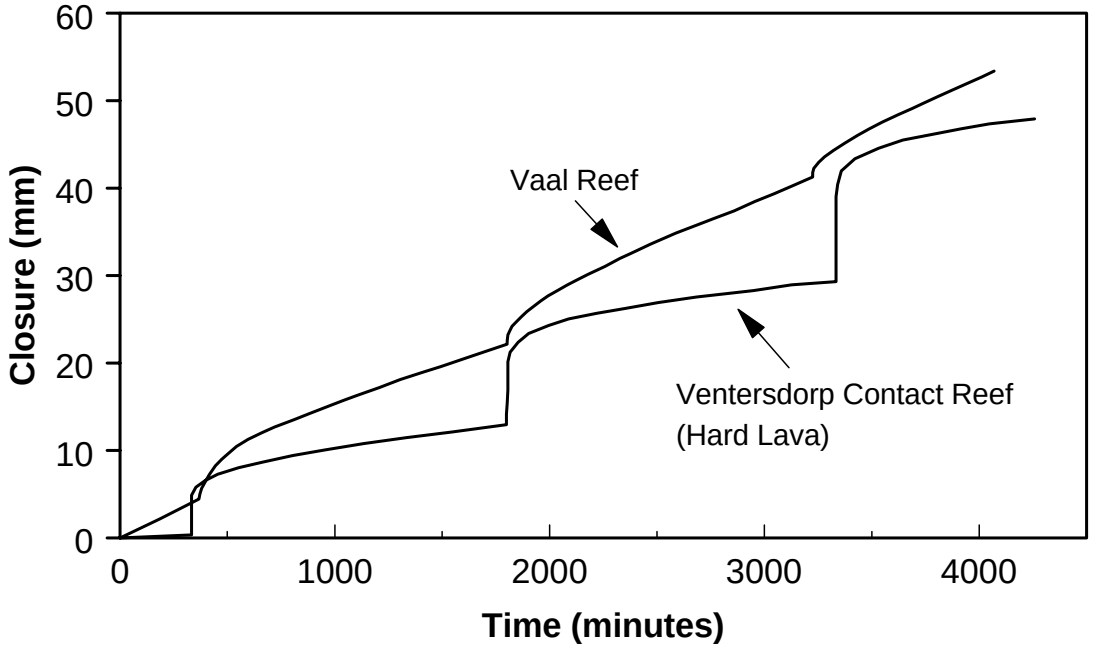

Figure 6. An example of continuous closure measurements in different geotechnical areas.

EFFECT OF MINING RATE ON RATE OF CLOSURE

Until recently, the effect of mining rate on the behaviour of the rock mass around deep excavations has been largely ignored. If the deformation of the rock mass was purely elastic (no time-dependent deformation), the effect of mining rate would not play any role. From Figure 6 it is, however, clear that time-dependent closure behaviour is very prominent in some areas of the mining industry. Mining rate will therefore play a significant role on the amount of closure acting on support units as explained below.

For support design, it is important to quantify the amount of closure that will act on a support unit from installation until it is a certain distance behind the face. This is illustrated in Figure 7. In this particular example, the support unit is installed 3 m from the face on a specific day. After a period of time, the face has been advanced by 5 m, putting the support unit at a distance of 8 m from the face. As the rate of closure contains a time-dependent component, which persists even if there is no mining activity, the total closure acting on this support unit will depend on the mining rate.

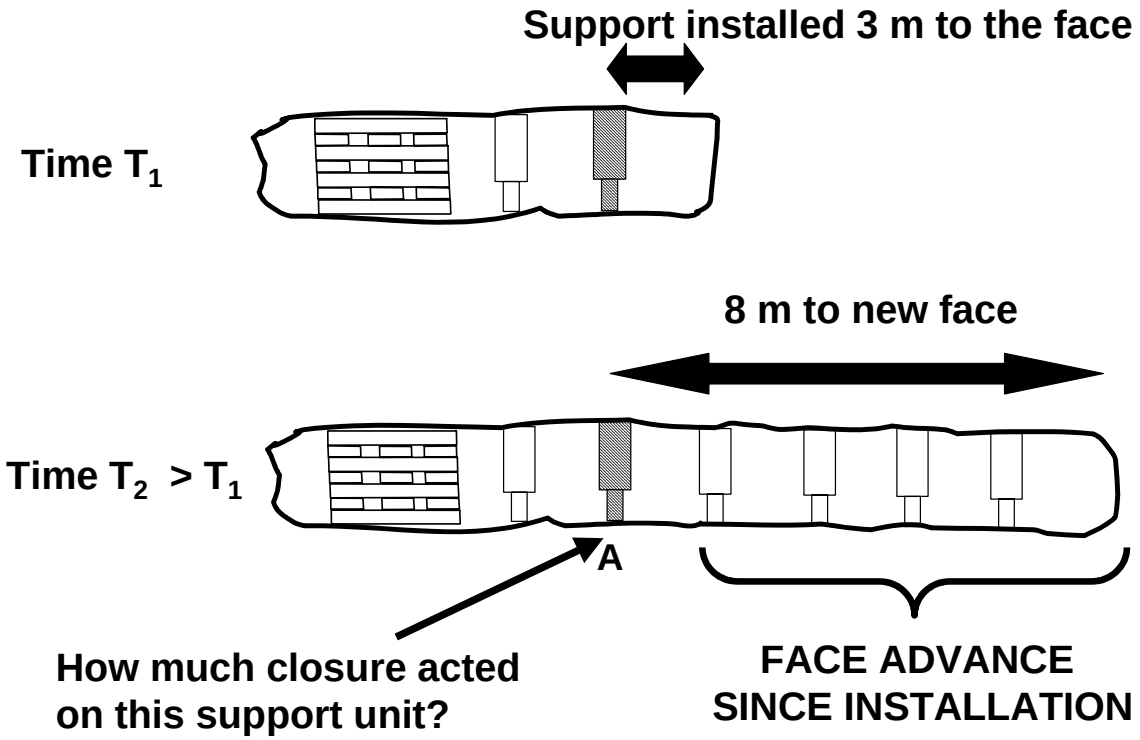

Figure 7. Example to illustrate the effect of mining rate on rate of closure.

The total daily closure, S^i_{daily}, acting on a support unit on a particular day i (where i = 1,2,3… to denote successive days) is given by the equation

$$S^i_{daily} = S^i_I + S^i_P + S^i_{SS} \qquad (2)$$

where S^i_I is the instantaneous closure, S^i_P is the primary closure phase and S^i_{SS} is the total steady-state closure for the particular day (see Figure 5). If there is no blasting (or no

large seismic events), the instantaneous and primary closure components are zero and equation (2) reduces to

$$S^{i}_{daily} = S^{i}_{SS} \tag{3}$$

For the example in Figure 7, the total closure can now be calculated for different mining rates. If blasting occurs every day (5 days to advance 5 m) the total closure acting on the support unit at the end of the fifth day is

$$S_{TOTAL} = \sum_{i=1}^{5} S^{i}_{daily} = \sum_{j=1}^{5} \left(S^{j}_{I} + S^{j}_{P} \right) + \sum_{i=1}^{5} S^{i}_{SS} \tag{4}$$

where j denotes each successive mining increment. The first term in equation 4 denotes the sum of the instantaneous and primary closure following each blast (assumed to be independent of mining rate) while the second term is the sum of the remaining time-dependent closure. If blasting, however, only occurs every second day (10 days to advance 5 m) the total closure acting on the support unit will be

$$S_{TOTAL} = \sum_{i=1}^{10} S^{i}_{daily} = \sum_{j=1}^{5} \left(S^{j}_{I} + S^{j}_{P} \right) + \sum_{i=1}^{10} S^{i}_{SS} \tag{5}$$

When comparing equations (4) and (5), it can be seen that the total closure acting on the support unit will be larger for the slower mining rate, even though the total face advance is 5 m in both cases. This has implications in that the slower mining rate will allow the energy absorption capability of a

given support unit to be eroded to a greater extent than if the mining rate was faster. A greater amount of the yieldability of the support is used up at the slower mining rate. Should a rockburst occur, the unit at point A in Figure 7 would have less ability to absorb energy as its remaining yieldability would be less than a unit at the same position where the mining was faster. Another phenomenon associated with slow mining rates is the unravelling of the hangingwall. It is well known that slow or intermittent mining rates lead to an unravelling of the hangingwall, thereby increasing the risks of falls of ground (COMRO, 1988). In light of the phenomena described above, it is therefore important not to leave faces standing or mine at very slow rates.

The difference in closure magnitude acting on the support unit for various mining rates will depend on the rate of steady-state closure. The larger the rate of steady-state closure, the bigger the effect of mining rate. When comparing the continuous closure profiles in Figure 6 for the different geotechnical areas, it can be seen that mining rate will play a bigger role on the Vaal Reef than the VCR (hard lava). A practical example to calculate rate of closure for different mining rates is given in Appendix A.

EFFECT OF MEASUREMENT POSITION ON CLOSURE BEHAVIOUR

When measuring rate of closure, the position of the closure instrument should always be recorded carefully. The distance to face is a very important parameter in this regard. For example, when calculating rate of closure, significantly different values can be obtained if the closure instrument was originally installed 3 m or 10 m from the face. This problem arises due to the special geometry of the tabular excavations where the incremental increase in closure after a blast can decrease very rapidly as the distance to face increases.

Effect of measurement position on elastic convergence

As a simple illustration of the effect of measurement position on closure, consider the incremental enlargement of an isolated stope with no total closure in the back area (Figure 8). The elastic convergence at certain fixed positions behind the original face will be calculated for an increase in span. This example is typical of underground closure measurements where the closure stations are installed a certain distance behind the face in stopes where the span has already reached a significant length. The amount of

closure prior to the installation of the closure meter is unknown and is taken as zero as a convenient reference level.

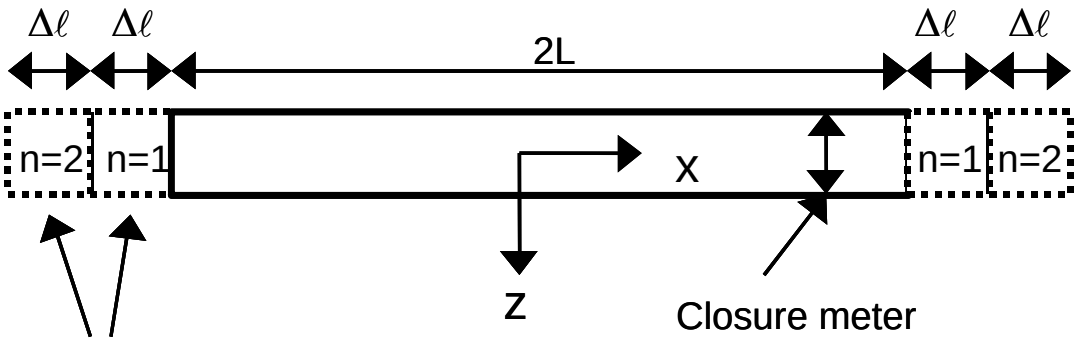

Figure 8. Incremental enlargement of a parallel sided stope panel. It is assumed that both sides of the stope are mined simultaneously. The closure meter is only installed after the stope has already reached a span of 2L.

The well-known two-dimensional elastic convergence solution of Salamon (1968), which is given in simplified form in Budavari (1983), gives the convergence for a stope of half-span L for cases where there is no total closure in the back area. This solution is for a stope where the entire span is excavated in one mining step. Further manipulation of this equation is therefore required to give the solution for the

incremental enlargement of the stope. This is illustrated in Appendix B. For a number of increments, n, the increase in closure at a fixed measuring point x is given by

$$\Delta S^{T} = \frac{4(1-\nu^2)W_z}{E}\left[\sqrt{(L+n\Delta\ell)^2 - x^2} - \sqrt{L^2 - x^2}\right] \qquad (6)$$

for $x \leq L$ and

$$W_z = \rho g H \qquad (7)$$

where 2L = span of the stope, ρ = density of the rock, g = gravitational acceleration, H = depth below surface, ν = Poisson's ratio, E = Young's modulus. As x is the distance from the centre of the stope, the distance from the measuring position to the face is given by

$$d = L + n\Delta\ell - x \qquad (8)$$

Equation (6) was plotted for a stope with an initial halfspan L = 150 m, Young's modulus = 70 GPa, Poisson's ratio = 0.2 for closure stations installed at 1 m, 5 m, 10 m and 20 m from the face. The face advance was 20 m on both sides. These results are plotted in Figure 9 with the average closure rate for each station also indicated in the figure. Note

that the rate of closure differs for the different positions. Imagine now that only a single closure station is installed at a distance of 5 m from the face. This will give an average closure rate of 7.46 mm/m after 20 m advance. If this rate is used to design a support unit installed 1 m from the face, the closure acting on the unit will be estimated to be 149.2 mm after a face advance of 20 m. From Figure 9, however, it is seen that the closure will be 191.2 mm.

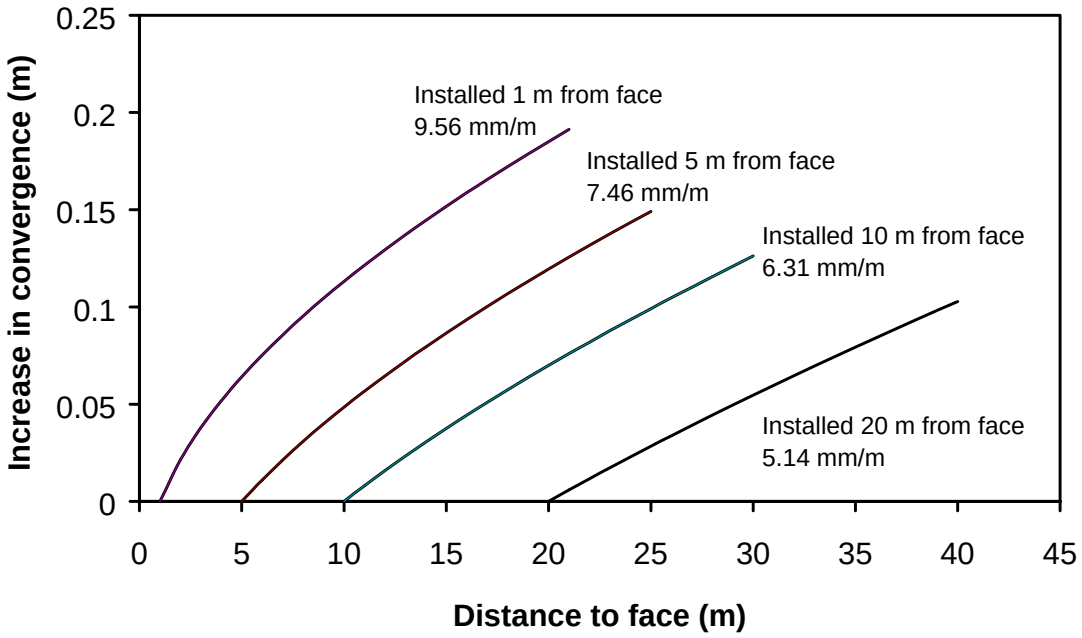

Figure 9. Effect of the measurement position (distance to face where the closure instrument is initially installed) on the convergence profiles and the calculated convergence rates. The face advance of 20 m was used in all four cases to calculate the average convergence rate in mm/m.

Underground examples of the effect of measurement position on closure

The previous section investigated the effect of distance to face on the amount of elastic convergence. The underground behaviour, however, includes inelastic behaviour and should therefore also be examined carefully. Malan (1998) collected some data on the effect of spatial position on closure behaviour for the SIMRAC project GAP332. Three closure meters were installed in an up-dip panel in a VCR (hard lava) stope (Figure 10).

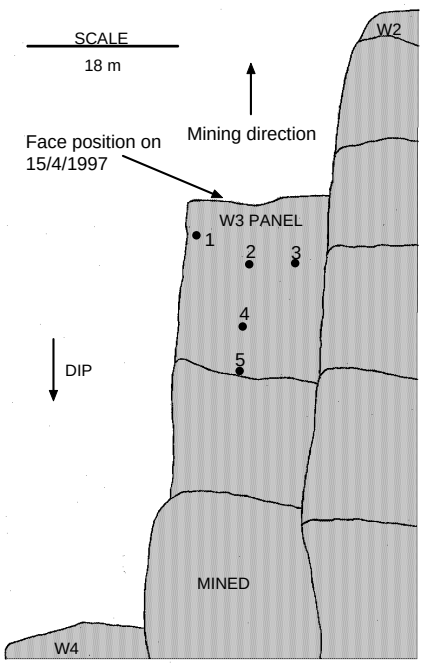

Figure 10. Plan view of the up-dip panel with the positions of the closure meters indicated (after Malan, 1998).

Figure 11 illustrates the incremental closure for stations 2, 4 and 5 after a particular blast. The primary closure is large close to the face, but decreases as the distance to the face increases. The rate of steady-state closure also decreases into the back area. Similar to the elastic convergence calculations above, it is found that the incremental increase in closure after a blast in the VCR stopes decreases with an increase in distance to face. Figure 12 compares the behaviour after the same blast for the row of stations parallel to the face (no. 1, 2 and 3). Although the steady-state closure rate is essentially similar for these three stations, the magnitude of primary closure increases from the tight (no. 1) to the loose ends (no. 3) of the panel.

For stiff environments such as the VCR with a hard lava hangingwall, it appears that the total closure in panels with large lead-lags is strongly affected by how close the point is to the abutment. For the high closure areas on the Vaal Reef, however, Roberts (2000) noted that the rate of closure at a specified distance to face is similar for points in the middle of the panel and close to the abutment. This was noted even for panels with large lead-lag distances. Malan (1998) also found that in some cases on the Vaal Reef, the

amount of steady-state closure can increase as the distance to face increases. This is shown in Figure 13.

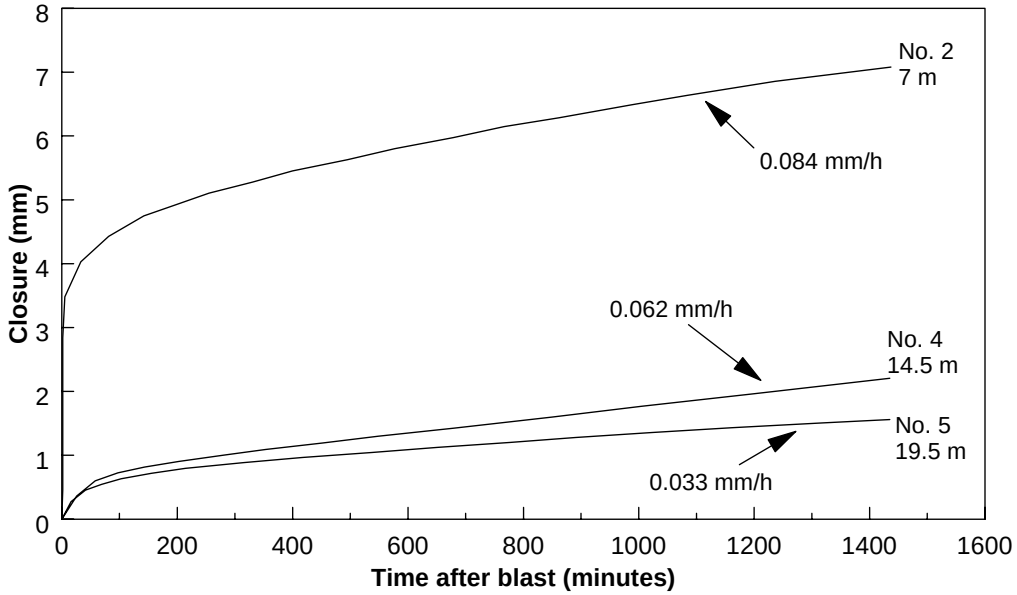

Figure 11. Closure as a function of time for different positions to the face following a blast.

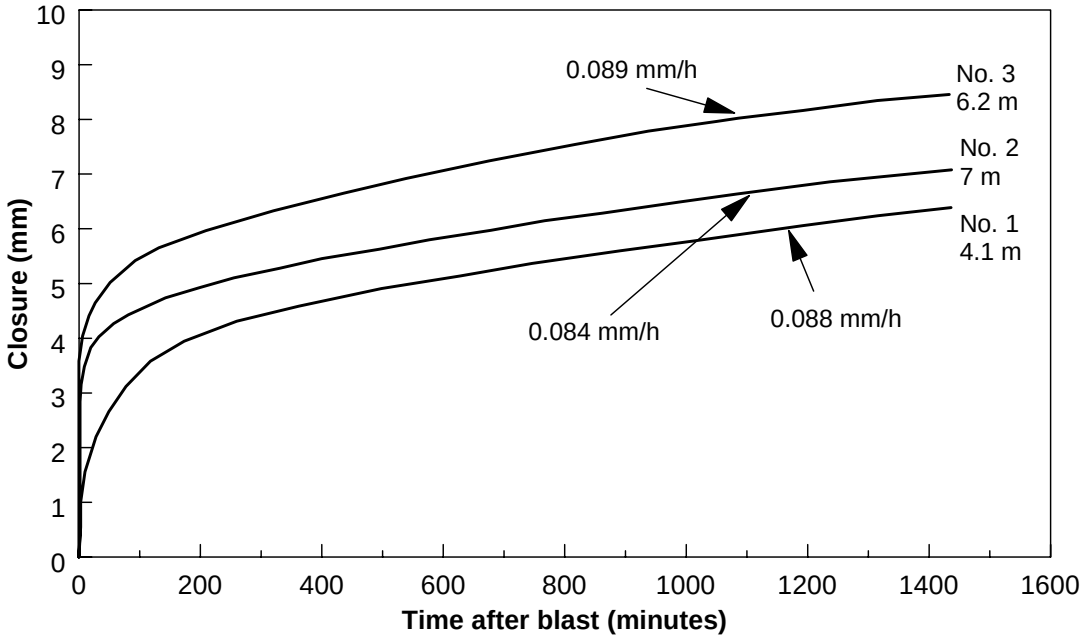

Figure 12. Closure as a function of time for different positions approximately parallel to the face following a blast.

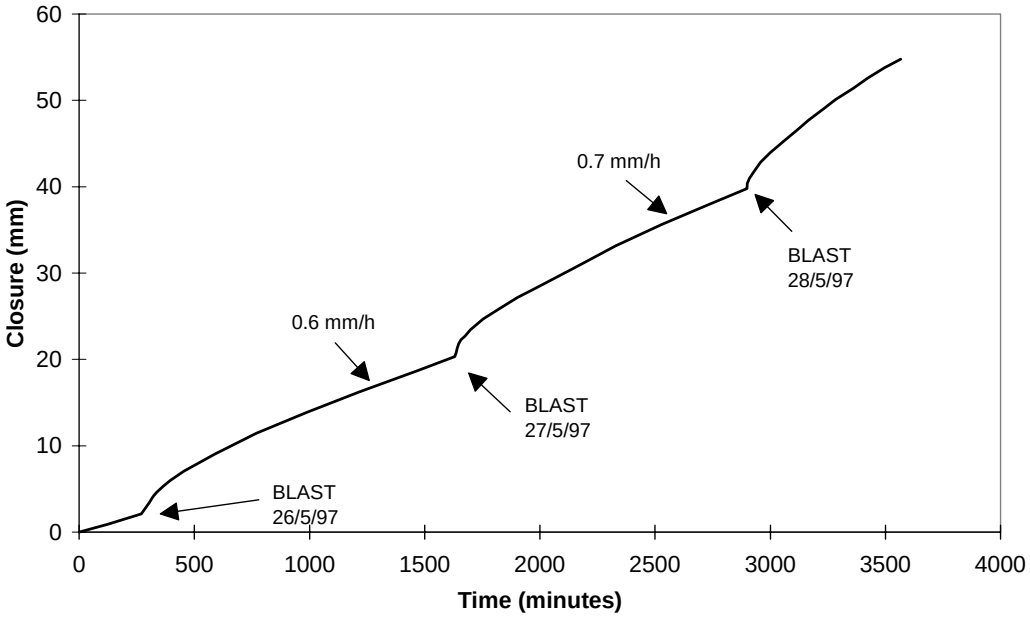

Figure 13. Closure measurements in a Vaal Reef stope for a larger distance to face than those in Figure 6. The instrument was 14.2 m from the face before the blast on 26/5/97.

EFFECT OF PRECONDITIONING ON CONTINUOUS CLOSURE BEHAVIOUR

Continuous closure measurements appear to be useful to measure the effectiveness of preconditioning. Figure 14 illustrates the effect of preconditioning on the closure behaviour of a VCR (hard lava) stope. Note that the steady-state closure rate increases significantly after the onset of preconditioning. This is further illustrated in Figure 15, which compares the rate of steady state closure as a function of distance from the face for the same area with and without preconditioning. These rates were calculated for 10 hours to approximately 24 hours after each blast. It is clear from this that the rate of steady-state closure is significantly increased by preconditioning. This is probably an indication of enhanced time-dependent deformation processes in the rock mass which reduces the amount of strain energy stored close to the face and, therefore, also reduces the likelihood of face bursting.

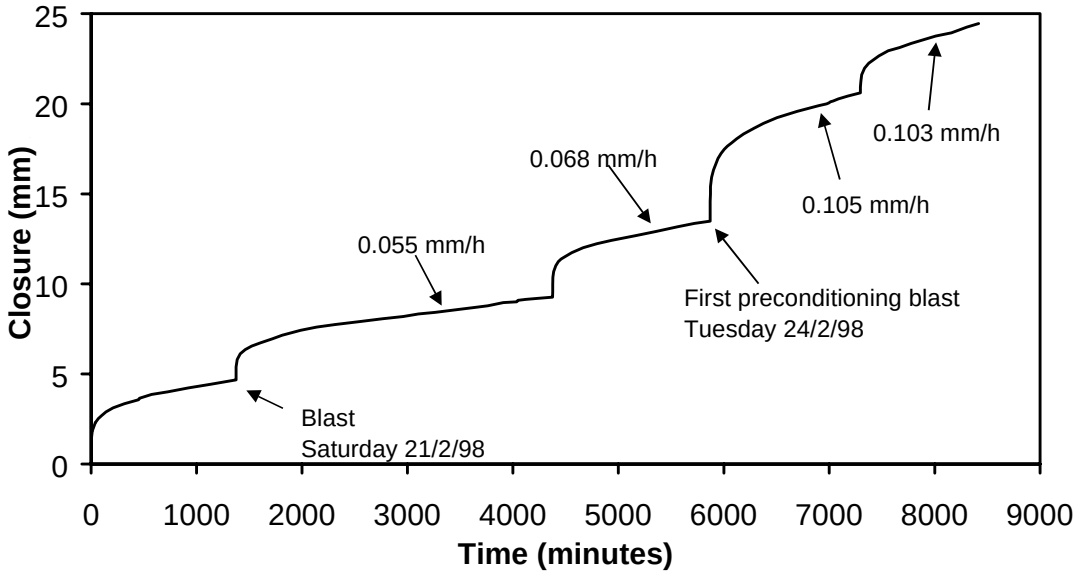

Figure 14. The effect of preconditioning on the closure behaviour of a VCR (hard lava) stope.

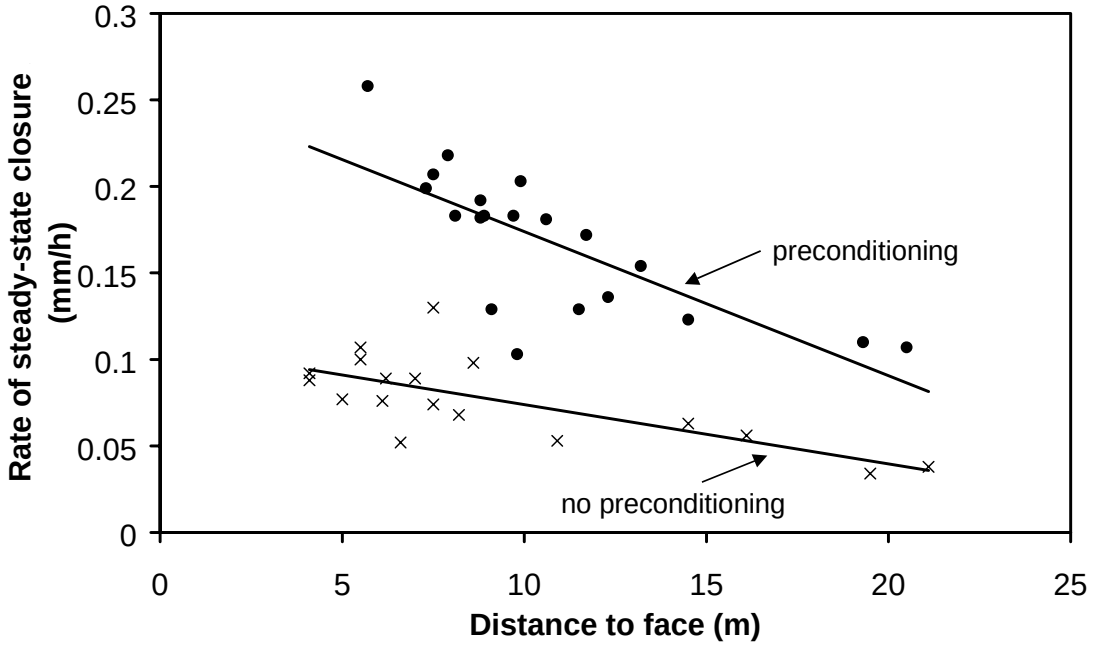

Figure 15. The effect of preconditioning on the rate of steady-state closure of a VCR (hard lava) stope.

CALCULATION AND USE OF THE CLOSURE RATIO

Definition of the closure ratio

A useful closure parameter is the closure ratio CR. For a single mining increment j, CR is defined as the ratio of instantaneous to total daily closure given by (from Figure 5)

$$CR_j = \frac{\Delta S_i^{\,j}}{\Delta S_T^{\,j}} \qquad (9)$$

For n successive blasts, the average closure ratio can be written as

$$CR = \frac{1}{n}\sum_{j=1}^{n} \frac{\Delta S_i^{\,j}}{\Delta S_T^{\,j}} \qquad (10)$$

The period Δt used for calculating ΔS_T is taken as 24 hours. In some cases, this period might be slightly shorter if the next blast occurs before the full 24 hours has expired since the previous blast. As it might be difficult in practice to determine the magnitude of the instantaneous closure from the graphs, it is suggested that $\Delta S_i^{\,j}$ be taken as the increase in closure during the 5 minute period following the blast.

Use of the closure ratio to identify geotechnical conditions and associated hazards

Figure 16 illustrates closure data collected in a VCR stope with a hard lava hangingwall. The competent lava has a strong influence on the closure behaviour and the general rock mass behaviour of these stopes. This particular area was prone to face bursting. When applying equation (10) to this data set, a closure ratio of CR = 0.46 is obtained. It should be noted that this is an average value as the closure ratio for the first blast is 0.36, the second 0.51 and the third 0.52. As a possible hazard parameter, it is therefore important not to focus on a single CR value after a particular blast, but rather an average over a period of time.

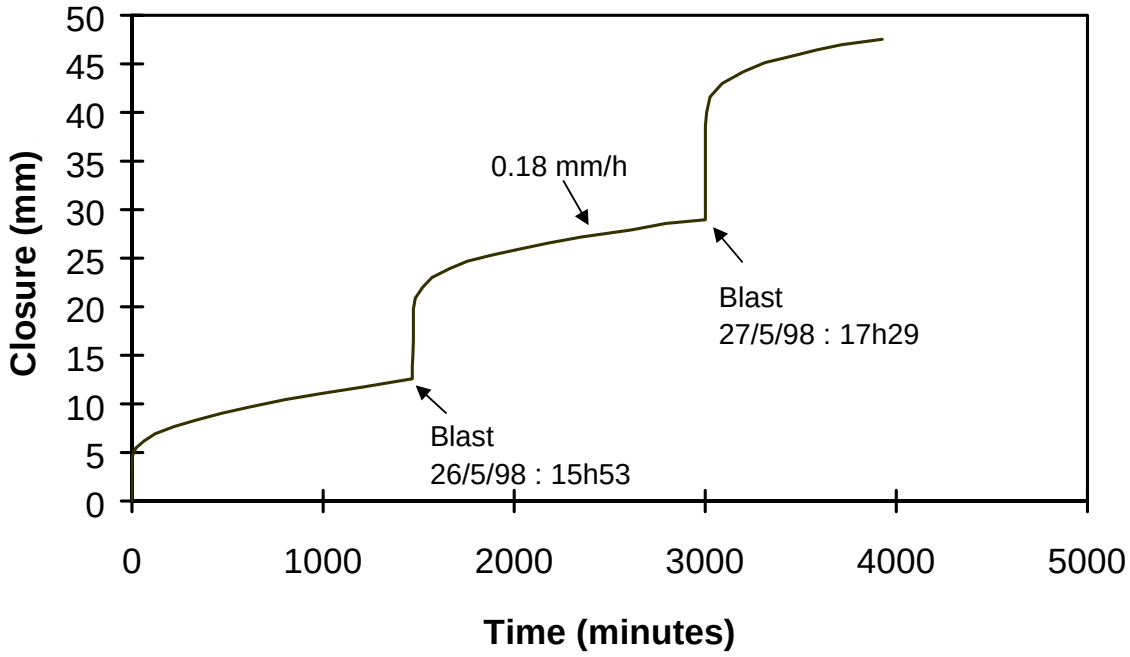

Figure 16. Time-dependent closure measured in a VCR stope where the hangingwall consists of hard lava (after Malan and Napier, 1999). The closure instrument was 8.1 m from the face before the blast on 26/5/98.

Continuous closure data was also collected at a different mine where the hangingwall of the VCR consisted of soft lava (Figure 17). The rock mass behaviour and the closure response in this area were dominated by the time-dependent disintegration of the soft lava in the hangingwall. It was very difficult to support the hangingwall, with significant fallouts occurring between packs. The risk of strain bursting was low in this area, although the risk of falls of ground was very high. When applying equation (10) to this data set, a closure

ratio of CR = 0.04 is obtained.

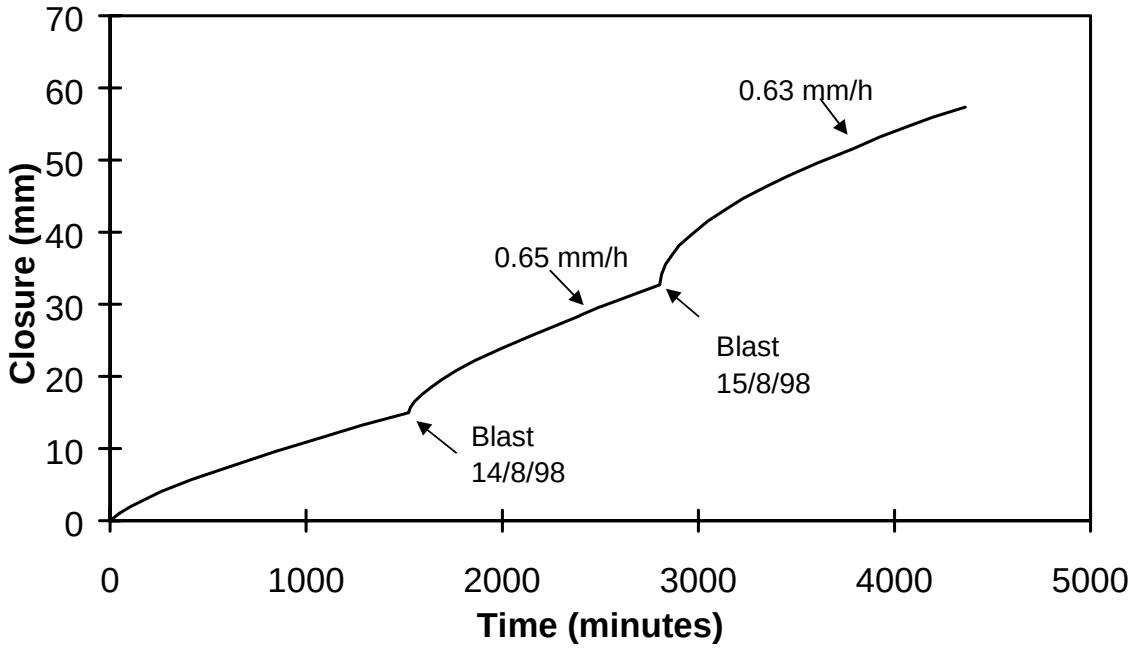

Figure 17. Time-dependent closure measured in a VCR stope where the hangingwall consisted of soft lava (after Malan and Napier, 1999). The closure instrument was 8.5 m from the face before the blast on 14/8/98.

Data from a third geotechnical area, the Vaal Reef, is shown in Figure 18. Well-defined bedding planes in the quartzite of the hangingwall dominate the rock mass behaviour and closure response of the stopes. These areas appeared to be prone to falls of ground while the risk of strain bursting was very low. When applying equation (10) to this data set, a

closure ratio of CR = 0.06 is obtained.

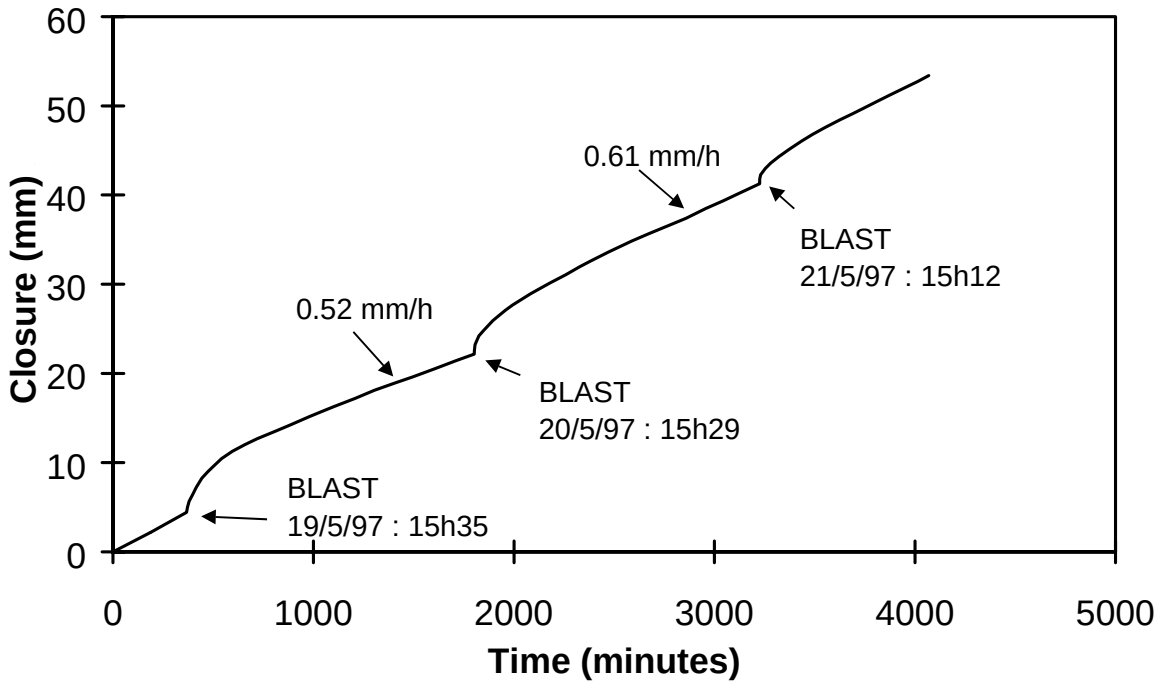

Figure 18. Closure measured in a Vaal Reef stope (after Malan and Napier, 1999). The instrument was 10.9 m from the face before the first blast.

From this data, it appears that the closure ratio is a good measure to identify different geotechnical conditions. The results are summarised in Table 1. Low values of closure ratio are typically associated with poor hangingwall conditions and a high risk of falls of ground whereas high values of closure ratio are associated with areas prone to face bursting. As mentioned above, however, the closure ratio does not stay constant for every blast but shows some

statistical variation. It is therefore important to calculate an average value and to use this as a base value to investigate possible changes in conditions in the stope over a period of time.

Table 1 Typical values of closure ratio for different geotechnical conditions.

Area	**Closure Ratio**	**Conditions**	**Reference**
1.VCR (hard lava)	0.46	High risk of face bursting, Significant seismicity,	Malan and Napier, 1999
2. VCR (soft lava)	0.04	Very high risk of falls of ground, low risk of strain bursting	Malan and Napier, 1999
3. Vaal Reef	0.06	High risk of falls of ground, low risk of strain bursting	Malan and Napier, 1999
4. Carbon Leader	0.35	Good backfill installation, stable hangingwall conditions, seismically active area	Malan et al, 1999
5. VCR (soft lava)	0.15	More stable hangingwall conditions than area no 2	Malan and Van Rensburg, 1999

INSTRUMENTATION TO MEASURE CONTINUOUS CLOSURE

As this guide focuses on continuous closure measurements, instrumentation commonly used to collect long term closure measurements such as spring vernier closure meters and four-peg closure ride stations will not be discussed in this guide. The reader is referred to Ryder and Jager 2002 for a description of these instruments and their use. The following is a list of some of the instruments used to collect continuous closure data. It should be noted that various companies are continually involved in the design of new closure meters and the following list is not exhaustive.

Clockwork closure meters

Although the clockwork closure meter is an old mechanical design, it is a reliable device and is still occasionally used to collect closure data. A benefit of this instrument is that it can be used in areas where intrinsically safe instruments are required. A drawback is that the data is collected on graph paper and significant effort is required to digitise and analyse the data. The mechanism of this instrument is shown in Figure 19.

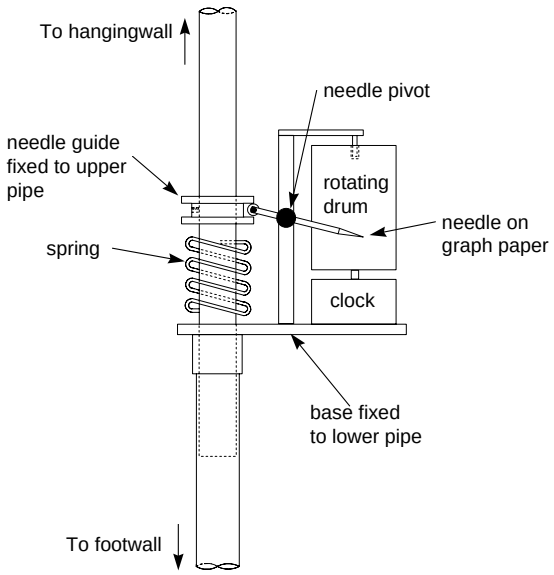

Figure 19. Mechanism of the clockwork closure meter.

The clockwork closure meter comprises two telescopic tubes with one of the tubes sliding against the pressure of a spring. The base of the instrument is fixed to the lower tube with the needle being moved by a guide fixed to the upper tube. The instrument is installed with the needle point close to the bottom of the graph paper on the drum. Stope closure moves the upper tube further into the lower tube with the needle point moving upwards on the paper. The clock typically rotates the drum once every seven days, resulting in a continuous record of closure over this period. The needle arm can be designed with various possible pivot points to allow for different amplification factors of the closure magnitude. Unfortunately this design is inherently

flawed as instantaneous closure is recorded as an arc, thereby distorting the time axis. The data needs to be corrected before use as indicated in Appendix C. An example of the raw data recorded on the graph paper is given in Figure 20. Figure 21 illustrates the same data after it was digitised and corrected according to the procedure in Appendix C.

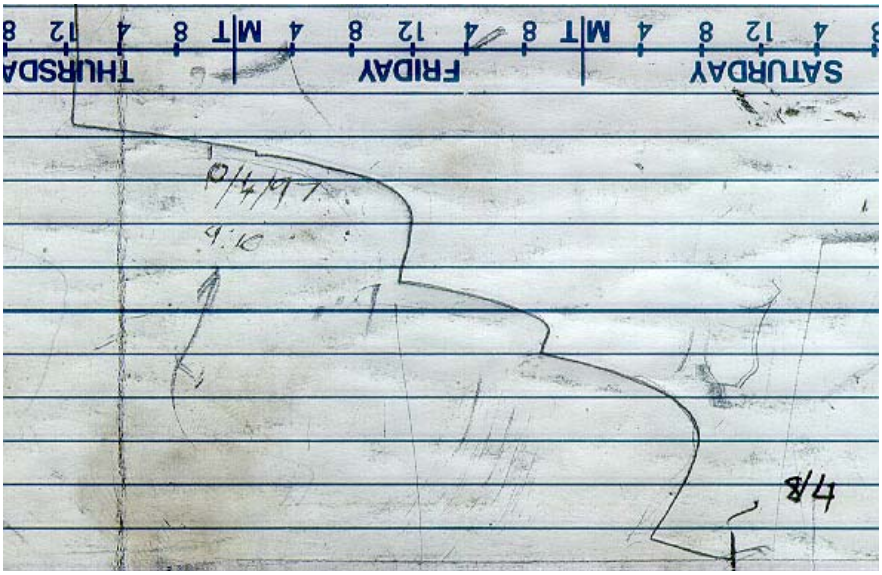

Figure 20. An example of continuous closure data recorded using the clockwork closure meter.

Figure 20 only shows a small section of the graph paper sheet and is not printed to scale. The horizontal grid lines are separated by a vertical distance of 5 mm. Note that the horizontal axis represents time, which increases to the left. The days printed on the paper indicate an increase of time to

the right, but this is incorrect as the paper was mounted upside down on the drum. The vertical axis represents closure magnitude which increases upwards. The pivoting needle arm resulted in the actual closure magnitude being multiplied by a factor of 1.86 on the graph paper.

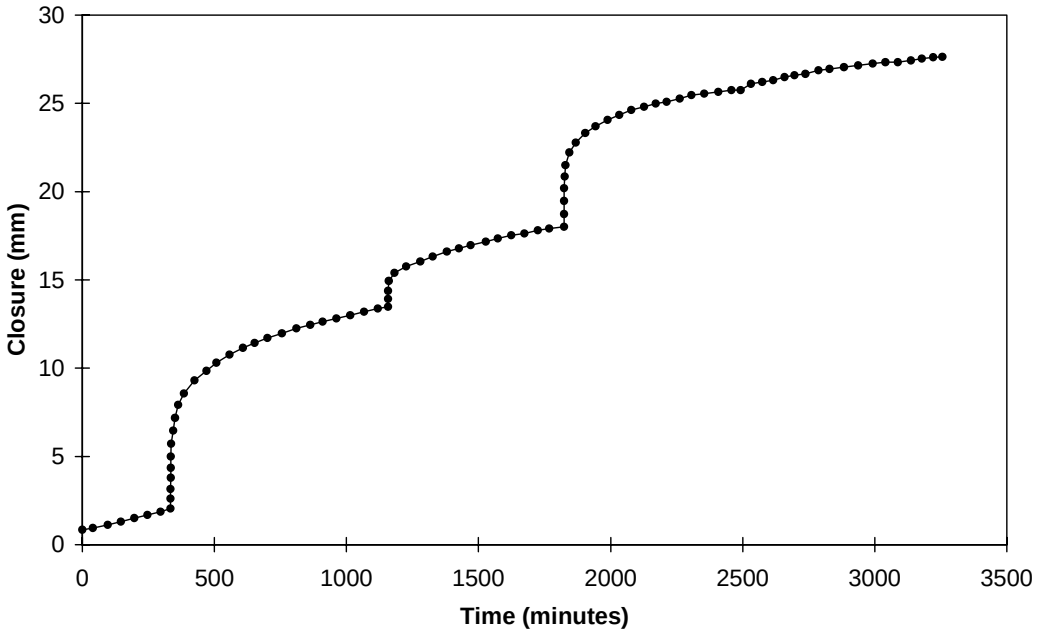

Figure 21. The corrected closure data for the measurements depicted in Figure 20. The data points give an indication of the digitisation interval used.

When installing the instruments underground, it is important that the two tubes make contact with solid rock in the hangingwall and footwall respectively. The tubes are typically secured to the hangingwall using quick-setting putty. When installed close to the face, the instrument

should be protected from blast damage by installing it behind support units. Figure 22 illustrates a typical installation underground.

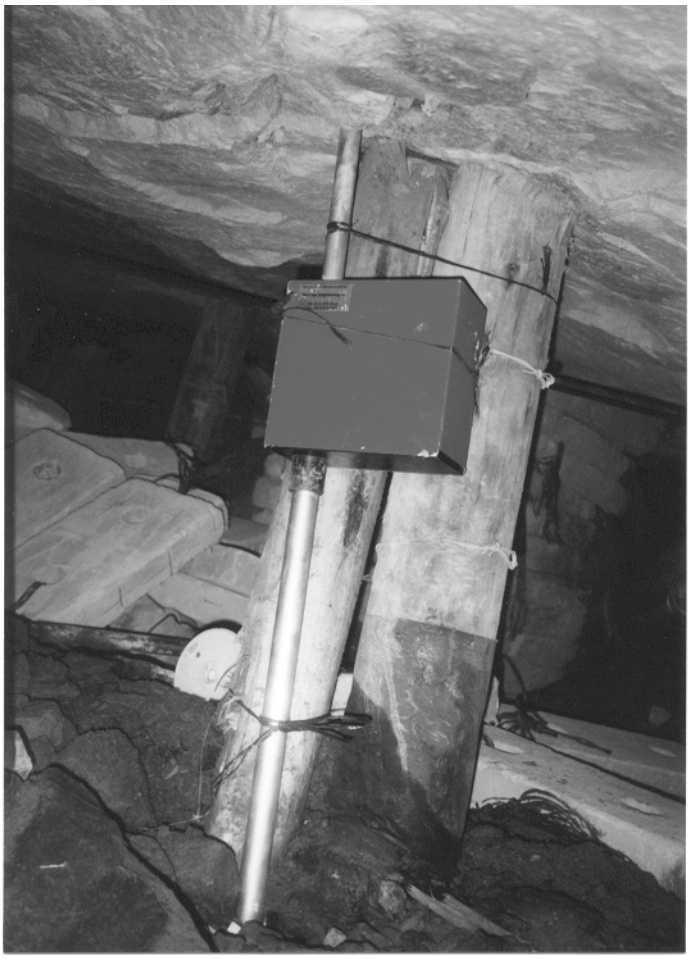

Figure 22. Installation of a clockwork closure meter in a stope. It is important when installing these meters that the lower tube makes contact with solid rock in the footwall.

In dipping stopes, the instruments should be installed normal to the plane of the reef to measure the closure component. It

should be noted that with time, a significant ride component will tilt the instrument, resulting in a composite measurement.

Potentiometer closure meter

These meters (also called wire-pull closure meters) consist of a multi-turn potentiometer which is bolted to the hangingwall (Figure 23). The wire is anchored in the footwall. Closure causes a change in electrical resistance of the potentiometer which, with the aid of a suitable interface, can be recorded using a data logger. Figure 24 illustrates a commercially available potentiometer closure meter.

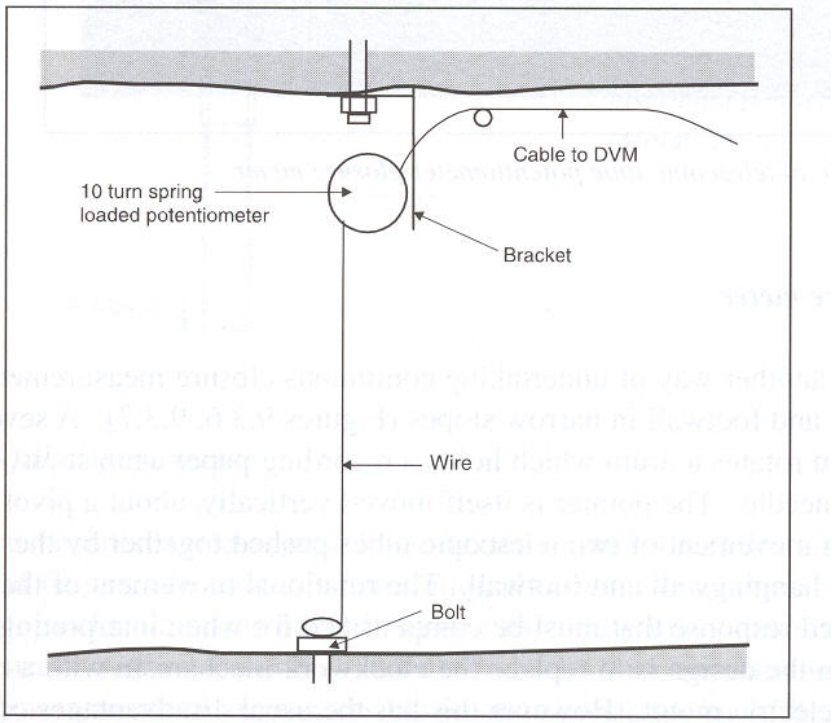

Figure 23. Schematic of a potentiometer closure meter (after Ryder and Jager, 2002).

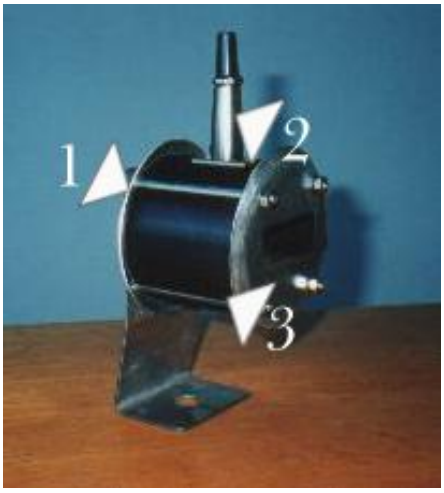

Figure 24. A wire-pull closure meter from Qualitec Engineering (courtesy Qualitec Engineering). The numbers refer to 1) stainless end plates and bracket, 2) Canon plug and socket and 3) Nylon body.

As the wire is prone to damage, a more robust design incorporates a potentiometer with a spring loaded telescopic steel tube (Figure 25). Figure 26 illustrates a typical installation underground.

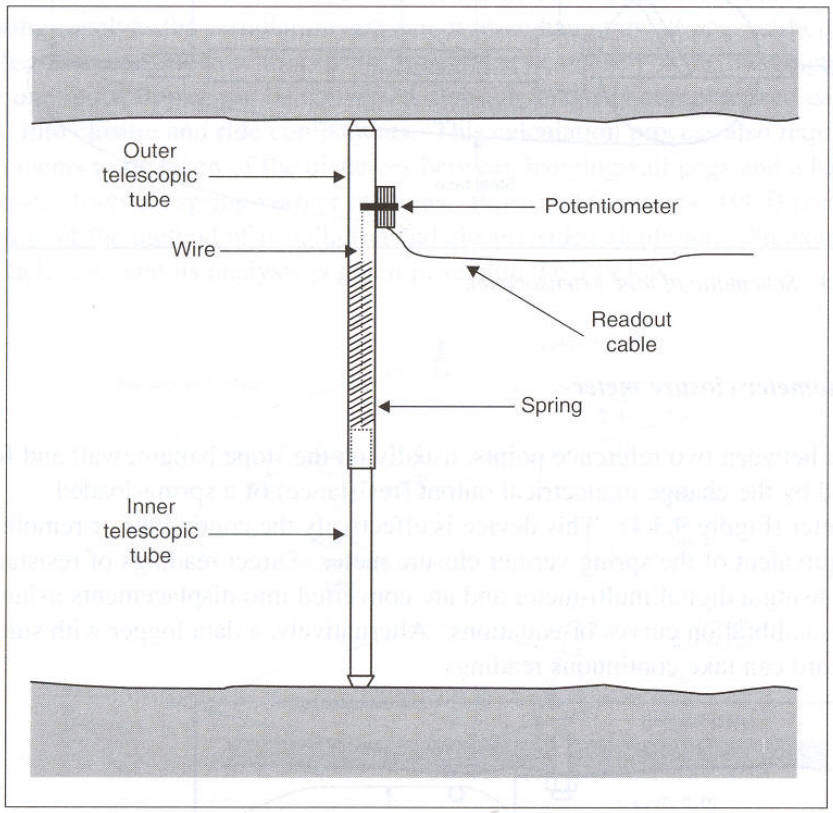

Figure 25. Schematic of a telescopic tube potentiometer closure meter.

Figure 26. A potentiometer closure meter integrated with a spring-loaded telescopic tube. Note the external logger used to collect the data.

New generation telescopic closure meters

A problem that is encountered when using closure meters with external loggers is that the cabling and connectors are prone to damage. A recent design philosophy is therefore towards more compact instruments where the transducer, datalogger and batteries are contained in a single telescopic

tube. These meters are easier to transport and to install. As an example, Figure 27 illustrates a closure meter designed by CSIR Miningtek. This design provides a relatively robust meter as all the electronic components, data logger and batteries are contained within the telescopic tubing. It is also lightweight, easy to install and to move as the main body of the meter is manufactured from rigid PVC piping. It allows a maximum deformation of 300 mm, and can be used in stope widths ranging from 990 mm up to 3 m by adding an additional section of PVC tubing. This is indicated in Figure 27b. This extension piece can be cut in the stope to the required length. A drawback is that these meters are not blast resistant and should be installed behind support units to protect them from damage. The data from these instruments can be downloaded underground with a handheld controller.

(a) (b)

Figure 27. (a) Telescopic closure meter developed at CSIR Miningtek and (b) installation underground.

GUIDELINES FOR CLOSURE MEASUREMENTS

- It is important to record the exact distance to face and measurement position in the stope when installing closure instruments. This information should be included in any report referring to the rate of closure.
- The rate of closure is very dependent on how close the instrument was initially installed from the face. This effect should be accounted for when designing stope support.
- When calculating rate of closure from long period measurements, it is important to record the exact time interval (for rates in mm/day) or distance interval (for rates in mm/m) used in the calculation.
- Continuous closure measurements should be recorded to establish the magnitude of the instantaneous closure response at blasting time and the rate of steady-state closure. The closure ratio should also be calculated. It is important to note that this information cannot be obtained from long period measurements.
- The rate of closure is very dependent on the mining rate. When collecting long period measurements, it is therefore important to note the mining rate. If stope support is designed using this rate, the design may not meet the

design criterion if there are significant changes in mining rate. Continuous closure measurements can be used to estimate how the rate of closure will be affected by mining rate (see Appendix A).

References

1. ISRM 1975
2. Wiggill, R.B. 1965. The effects of different support methods on strata behaviour around stoping excavations. *Symposium on Rock Mechanics and Strata Control in Mines: J. S. Afr. Inst. Min. Metall.*: 1-35.
3. Gürtunca R.G. & Adams D.J. 1991. Determination of the in situ modulus of the rockmass by the use of backfill measurements. *J. S. Afr. Inst. Min. Metall*. 91(3): 81-88.
4. COMRO 1988. An industry guide to methods of ameliorating the hazards of rockfalls and rockbursts.
5. Salamon, M.D.G. 1968. Two-dimensional treatment of problems arising from mining tabular deposits in isotropic or transversely isotropic ground*. Int. J. Rock Mech. Min. Sci.,* 5: 159-185.
6. Budavari, S. 1983. *Rock mechanics in mining practice*. SAIMM Monograph Series M5: Johannesburg.
7. Malan, D.F. 1998. An investigation into the identification and modelling of time-dependent behaviour of deep level excavations in hard rock. *PhD Thesis*, University of the Witwatersrand, Johannesburg.
8. Malan, D.F. and Napier, J.A.L. 1999. The effect of geotechnical conditions on the time-dependent behaviour of hard rock in deep mines. In: Amadei, B., Kranz, R.L., Scott, G.A. and Smeallie, P.H. (eds.) *37th U.S. Rock Mechanics Symposium*, Vail Rocks ’99, pp. 903-910, Balkema.
9. Malan, D.F., Janse Van Rensburg, A.L. and Ozkaya, D. 1999. Continuous closure behaviour of the Carbon Leader Reef at Western Deep Levels Mine (East Shaft). Internal report submitted to mine.
10. Malan, D.F. and Janse van Rensburg, A.L. Continuous closure measurements at Kloof Mine: 37-61 longwall Main shaft. Internal report submitted to mine.
11. Ryder, J.A. and Jager, A.J. 2002. A textbook on rock mechanics for tabular hard rock mines. SIMRAC.

APPENDIX A

Estimating rate of closure for different mining rates

The rate of closure can be estimated for different mining rates provided enough continuous closure data is collected at various distances from the stope face. The following steps should be followed:

STEP 1 (calculate the daily rate of closure with blasting)

From the continuous closure measurements, the rate of closure following a regular blast in a 24 hour period should be quantified. As an example, from the data in Figure A1, the total closure following the blast is 13 mm. Assuming the face advance after this blast is 0.8 m, the rate of closure is 13 mm / 0.8 m = 16.3 mm/m. This particular data set was obtained in a VCR (hard lava) up-dip panel in the Carletonville area. These calculations should be repeated for different blasts and different distances to face to get an average value of closure rate for specified distances to face.

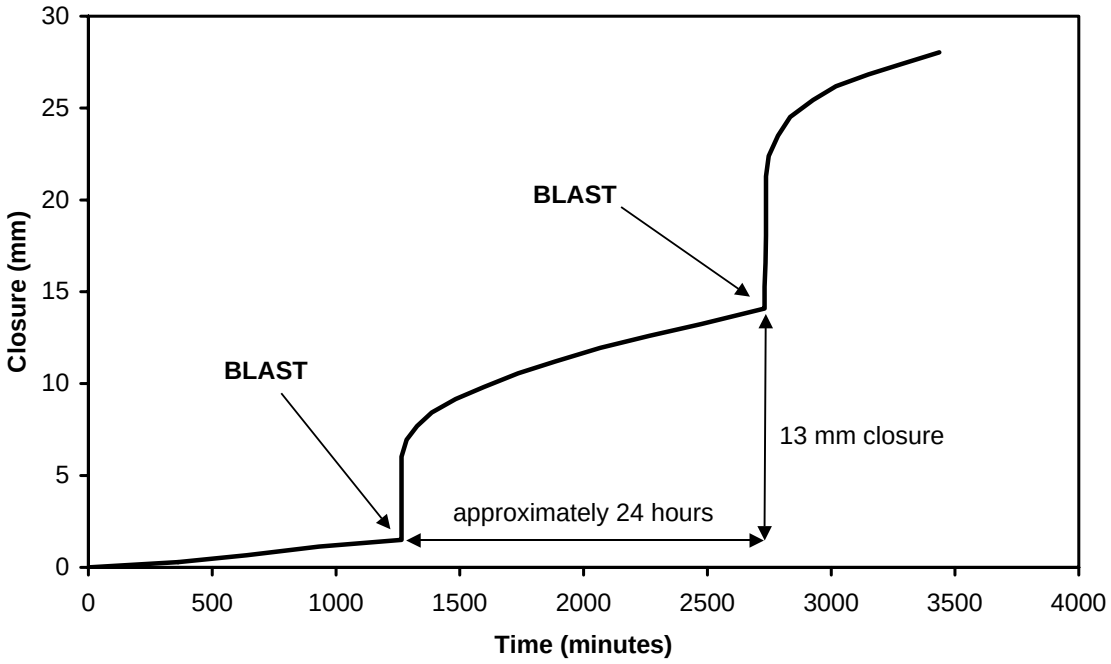

Figure A1. Calculation of the rate of closure in the 24 hours following a blast. This closure was measured at a distance of 8 m to the face.

STEP 2 (quantify the decrease in steady-state closure in the absence of blasting)

Examine the nature of the steady-state closure. As mentioned in the section on terminology, the rate of steady-state closure appears to be constant in the short term but it gradually decreases if there is no blasting or seismic activity. This is illustrated in Figure A2. The measurements were obtained over a long weekend when there was no mining activity for several days.

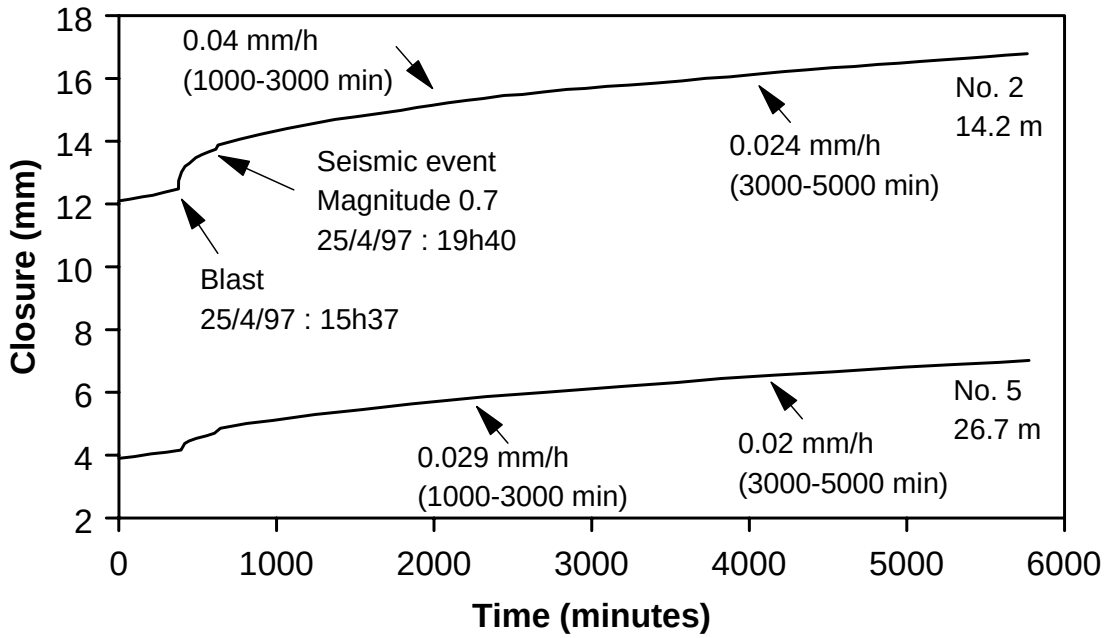

Figure A2. Closure measured in a VCR (hard lava) panel when there was no mining activity for a period of four days. The time periods in brackets indicate the intervals used to calculate the rates of steady-state closure. Two closure instruments at different distances to the face were used to collect the data (after Malan, 1998).

The steady-state closure is best approximated by a function of the form

$$\Delta S_{SS} = a\left(1 - e^{-bt}\right) \qquad \text{(A1)}$$

where a and b are parameters and t is time. The steady-state closure for Station No. 2 in Figure A2 after the seismic event was plotted in Figure A3 together with the model given

in equation (A1). The parameters used to obtain this fit were a = 3.85 mm and b = 0.015 h^{-1}. Note that these values are only applicable to this particular stope.

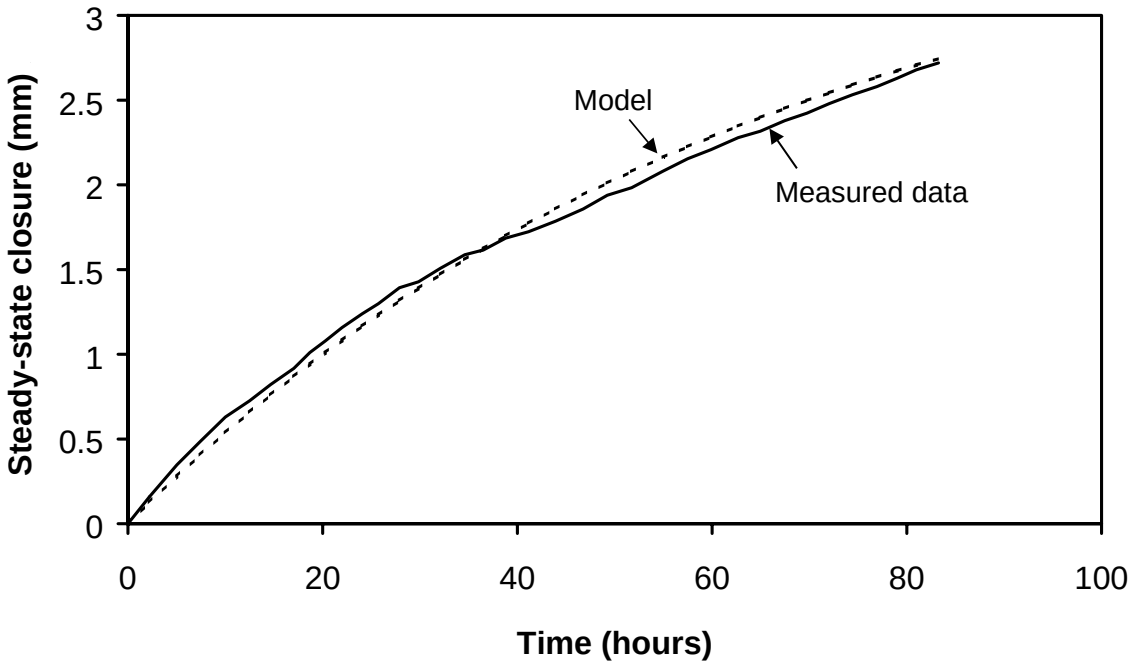

Figure A3. Measured and simulated values of steady-state closure for the VCR (hard lava) panel.

From equation (A1), the rate of steady-state closure is given by

$$\frac{dS_{SS}}{dt} = ce^{-bt} \qquad \text{(A2)}$$

where

$$c = ab \qquad \text{(A3)}$$

From equation (A2), the rate of steady-state closure at t = 0 is given by c. For convenience, equation (A1) will be written as

$$\Delta S_{SS} = \frac{c}{b}\left(1 - e^{-bt}\right) \qquad \text{(A4)}$$

STEP 3 (quantify the effect of distance to face)

As mentioned above, the rate of steady-state closure is also a function of the measurement position in the panel. This is indicated in Figure A4 where the rate of steady-state closure appears to decrease as the distance to face increases. The parameter c in equation (A4) is therefore a function of the distance to face. As the rate of steady-state closure is also a function of the length of face advance on a particular day and the position in the panel along strike, there is some scatter present in the data as illustrated in Figure A4. The parameter c will therefore be approximated by the following function

$$c = \alpha e^{-\beta d} \qquad \text{(A5)}$$

where d is the distance to face. From the fit in Figure A4, calibrated values for α and β are 0.1195 mm/h and 0.0454 m^{-1}, respectively. Inserting equation (A5) in (A4) gives

$$\Delta S_{SS} = \frac{\alpha e^{-\beta d}}{b}\left(1 - e^{-bt}\right) \qquad \text{(A6)}$$

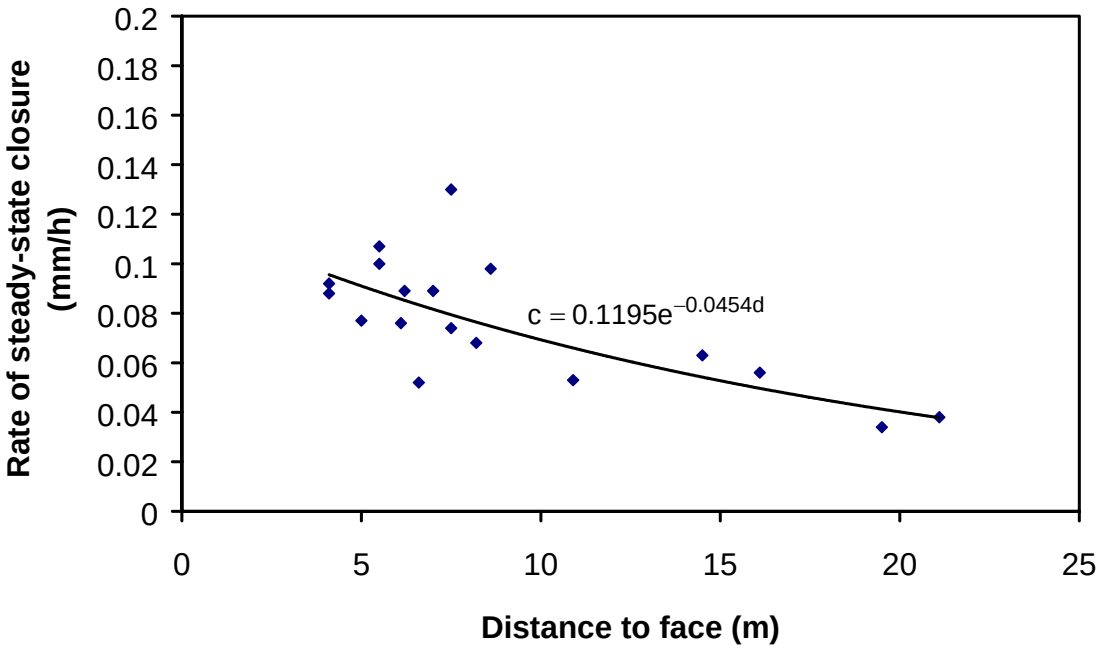

Figure A4. Effect of distance to face on the rate of steady-state closure. Although there is some scatter present in the data with a resulting poor fit to the given function, it will be used as a useful approximation of the trend.

STEP 4 (calculate the effect of mining rate on steady state closure)

As the decrease in rate of steady-state closure illustrated in Figure A3 is repeated after every blast, equation (A6) should be further modified to allow for the incremental enlargement

of the stope. If a closure meter is installed at a fixed position in the stope and a number of increments are mined, the total amount of steady-state closure measured at that position will be given by

$$S_{SS}{}^{T} = \sum_{k=1}^{n} \frac{\alpha e^{-\beta(k\Delta\ell+f)}}{b}\left[1 - e^{-b(\tau_k - \tau_{k-1})}\right] \qquad \text{(A7)}$$

where n is the number of mining increments and τ_k is the time when the k^{th} increment is mined. The distance to face is given by

$$d = k\Delta\ell + f \qquad \text{(A8)}$$

where $\Delta\ell$ is the size of each mining increment and f is the original distance to face.

Equation (A7) can now be used to simulate the effect of different mining rates on the steady-state closure at a specified measuring point behind the original face. An example is shown in Figure A5 for a support unit originally installed 5 m from the face and a face advance of 20 m. The size of each mining increment was assumed to be 1 m. The calibrated values for α, β and b obtained from Figures A3 and A4 were used. It is assumed that the parameters α and β are not functions of the mining rate. The effect of different

mining rates is clearly visible in Figure A5. It should be emphasised that the closure plotted in Figure A5 is only the steady-state closure and does not include the instantaneous or primary closure components. It is assumed that the cumulative contributions of the instantaneous and primary closure phases are not affected significantly by mining rate.

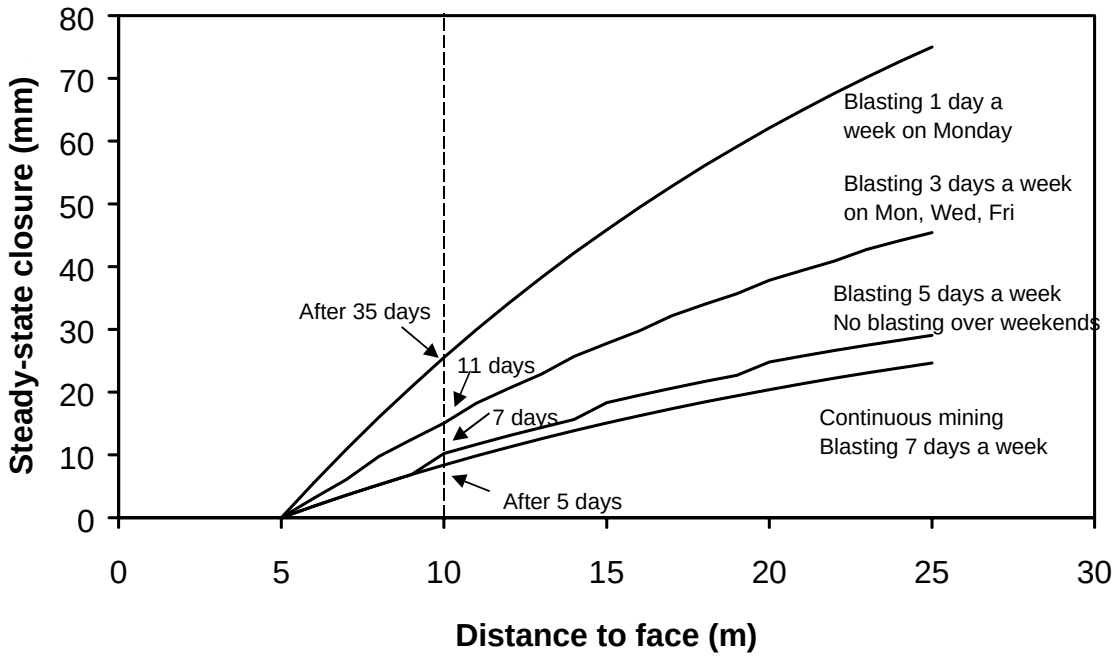

Figure A5. The effect of mining rate on the total amount of steady-state closure at a particular point in the stope.

STEP 5 (calculate the effect of mining rate on rate of total closure)

The rate of total closure can now be estimated from Figure A5. For a support installed 5 m from the face, the time-

dependent closure acting on it after a face advance of 5 m will be 8.4 mm for continuous mining.

- If mining takes place only 5 days a week, the time-dependent closure will be 10.2 mm. The difference is 1.8 mm or an extra time-dependent closure rate of 0.4 mm/m (1.8 mm/5 m). This extra 0.4 mm/m is added to the 16.3 mm/m from STEP 1 to give **16.9 mm/m.**

- If mining takes place only 3 days a week, the extra time-dependent closure will be 15.1 mm. The difference is 6.7 mm or an extra time-dependent closure rate of 1.3 mm/m (6.7 mm/5 m). This extra 1.3 mm/m is added to the 16.3 mm/m from STEP 1 to give **17.6 mm/m.**

- If mining takes place only 1 day per week, the extra time-dependent closure will be 25.5 mm. The difference is 17.1 mm or an extra time-dependent closure rate of 3.4 mm/m (17.1 mm/5 m). This extra 3.4 mm/m is added to the 16.3 mm/m from STEP 1 to give **19.7 mm/m.**

APPENDIX B

Elastic convergence solution for the incremental enlargement of a stope

The elastic convergence (S_z) of a horizontal (dip = 0º) parallel-sided panel in isotropic ground without contact between the hangingwall and footwall is given as (Salamon, 1968)

$$S_z^{(0)}(x) = \frac{4(1-\nu^2)W_z}{E}\sqrt{L^2 - x^2} \qquad \text{(B1)}$$

for $x \leq L$ where

$$W_z = \rho g H \qquad \text{(B2)}$$

and 2L = span of the stope, ρ = density of the rock, g = gravitational acceleration, H = depth below surface, ν = Poisson's ratio, E = Young's modulus and x is the distance from the centre of the stope.

Consider the incremental enlargement (both sides of the stope are simultaneously mined) of a stope as indicated in

Figure 8. The convergence of the original stope of half-span L is given by equation (B1). After mining an increment $\Delta\ell$ on both sides, the convergence is given by

$$S_z^{(1)}(x) = \frac{4(1-\nu^2)W_z}{E}\sqrt{(L+\Delta\ell)^2 - x^2} \quad \text{for} \quad x \le L + \Delta\ell \tag{B3}$$

The increase in closure after one increment is therefore

$$\begin{aligned}\Delta S_1 &= S_z^{(1)}(x) - S_z^{(0)}(x) \\ &= \frac{4(1-\nu^2)W_z}{E}\left[\sqrt{(L+\Delta\ell)^2 - x^2} - \sqrt{L^2 - x^2}\right] \quad \text{for} \quad x \le L\end{aligned} \tag{B4}$$

When mining a second increment, the total closure is given by

$$\begin{aligned}&S_z^{(2)}(x) = \frac{4(1-\nu^2)W_z}{E}\sqrt{(L+2\Delta\ell)^2 - x^2} \\ &\text{for} \quad x \le L + 2\Delta\ell\end{aligned} \tag{B5}$$

The new increment in closure caused by this second mining step is given by

$$\Delta S_2 = S_z^{(2)}(x) - S_z^{(1)}(x)$$
$$= \frac{4(1-\nu^2)W_z}{E}\left[\sqrt{(L+2\Delta\ell)^2 - x^2} - \sqrt{(L+\Delta\ell)^2 - x^2}\right] \quad \text{(B6)}$$
$$\text{for} \quad x \le L + \Delta\ell$$

The total increment in closure caused by these two mining steps is

$$\Delta S^T = \Delta S_1 + \Delta S_2$$
$$= \frac{4(1-\nu^2)W_z}{E}\left[\sqrt{(L+2\Delta\ell)^2 - x^2} - \sqrt{L^2 - x^2}\right] \quad \text{(B7)}$$

Similarly, for any number n of mining increments, it can be shown that the increment in closure is given by

$$\Delta S^T = \frac{4(1-\nu^2)W_z}{E}\left[\sqrt{(L+n\Delta\ell)^2 - x^2} - \sqrt{L^2 - x^2}\right] \quad \text{(B8)}$$
$$\text{for} \quad x \le L$$

APPENDIX C

Correction procedure for the clockwork closure meter data

As the design of the instrument is such that instantaneous closure is recorded as an arc (Figure C1), the time scale is distorted and the data needs to be corrected.

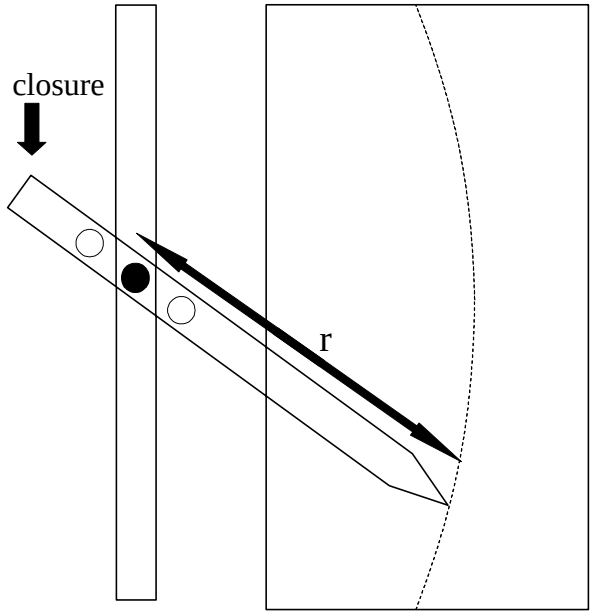

Figure C1. Recording mechanism of the clockwork closure meter. The particular setting of the needle arm for the meters results in the closure being amplified by a factor of m on the drum.

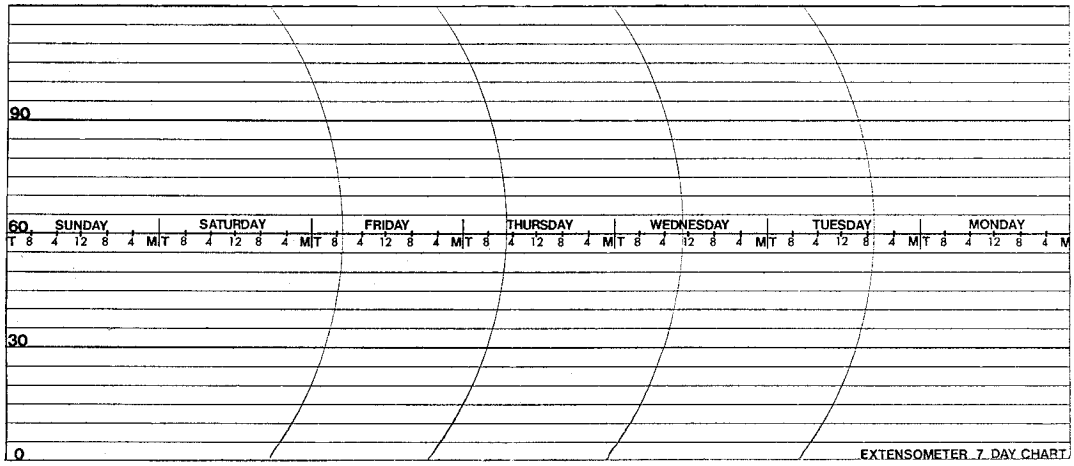

Figure C2. Sample of the calibration curves of a clockwork closure meter (not to scale).

For the correction procedure, the radius r needs to be determined. Although this can be directly measured at the instrument, it can also be calculated from the calibration curves in Figure C2.

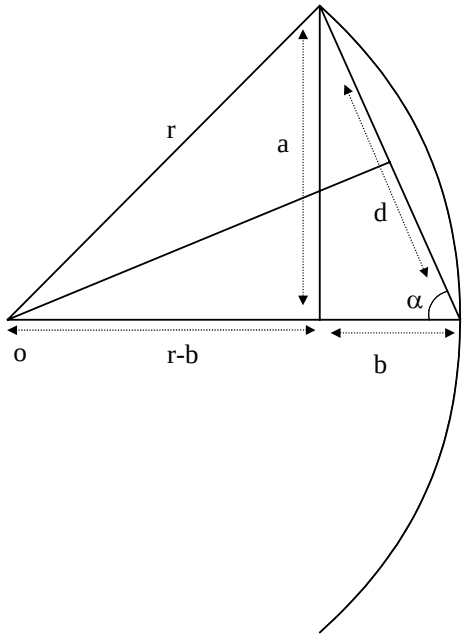

Figure C3. Calculation of the radius r from the calibration curves.

From Figure C3

$$r^2 = a^2 + (r - b)^2 \qquad \text{(C1)}$$

$$r^2 = a^2 + r^2 - 2rb + b^2 \qquad \text{(C2)}$$

$$r = \frac{a^2 + b^2}{2b} \qquad \text{(C3)}$$

For correction of the data, it is assumed that the x-values along the horizontal line in the centre of the graph paper (marked 60, Figure C2) is correct. Any deviation from this

line gives an error in x-value, $C_x(y)$, which becomes progressively worse as the distance from this line increases (Figure C4).

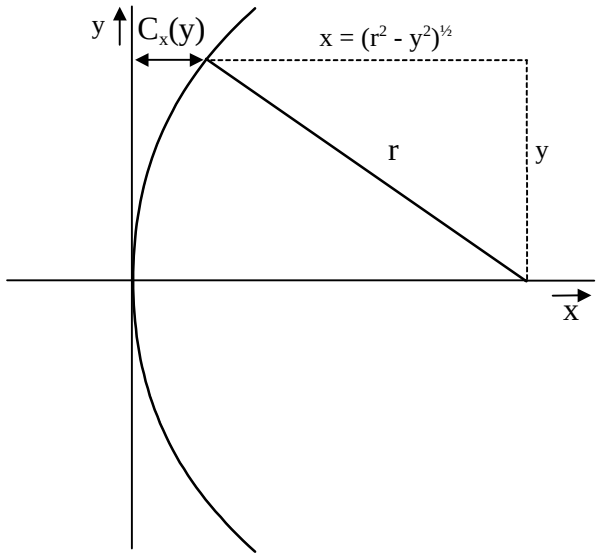

Figure C4. Illustration of the error in x-value as the curve deviates from the central horizontal line. The construction of the meter and the rotation of the drum are such that time (x-axis) increases away from the concave part of the arc.

The equation of the circle is given by $x^2 + y^2 = r^2$ or $x = \sqrt{r^2 - y^2}$ and therefore the error in x-value as a function of y is given as

$$C_x(y) = r - \sqrt{r^2 - y^2} \qquad \text{(C4)}$$

For a list of faulty data points (x_{old}, y_{old}) each data point should be corrected according to

$$x_{new} = x_{old} - C_x(y) = x_{old} - \left(r - \sqrt{r^2 - y_{old}^{\ 2}}\right) \qquad \text{(C5)}$$

$$y_{new} = \frac{y_{old}}{m} \qquad \text{(C6)}$$

where m is the closure amplification factor (see Figure C1).

As a first step in the correction procedure, the data must be digitised and any commercial package can be used. The data can then be corrected according to equations (C5) and (C6).